appropriate ratios of the elements, a stepwise synthesis based on $B_{12}X_{12}^{-2}$ and a thermal reaction of BI_3 in the presence of Si are experimental possibilities towards stuffed fullerenes. We refrain from speculating on the properties of these highly dense molecules.

In summary, it should be possible to stuff fullerenes by covalently bound units. Electron counting and overlap arguments help in selecting the right stuffing.

1 Taylor, R and Walton, D R M , *Nature*, 1993, **363**, 685–693.
2 Rao, C N R (ed), Special issue on fullerenes, *Indian J. Chem* , 1992, **31**
3 Kroto, H W , Allaf, A. W and Balm, S P , *Chem. Rev* , 1991, **91**, 1213–1235
4 Weiske, T , Wong, T , Kraitschmer, W , Terlouw, J K and Schwarz, H , *Angew Chem Int Ed Engl* , 1992, **31**, 183–185.
5. Saunders, M., *Science*, 1993, **259**, 1428–1430.
6 Saunders, M , Jimenez-Vazquez, H A , James Cross, R., Mroczkowski, S , Freedberg, D I. and Anet, F A. L., *Nature*, 1994, **367**, 256–259
7. Jemmis, E. D and Schleyer, P V. R , *J. Am Chem Soc.*, 1982, **104**, 4781–4788.
8 Giordano, C , Heldeweg, R F. and Hogeveen, H , *J Am Chem. Soc* , 1977, **99**, 5181–5184
9 Jutzi, P and Seufert, A , *Angew Chem* , 1977, **89**, 330–332
10 Pasinski, J P and Beaudet, R H , *J Chem Phys* , 1974, **61**, 683–691
11 Hammond, G S and Kuck, V J (eds), *Fullerenes Synthesis, Properties and Chemistry of Large Carbon Clusters*, ACS Symposium Series, vol 481, American Chemical Society, Washington, DC, 1992
12 Guo, T , Jin, C and Smalley, R E., *J. Phys Chem* , 1991, **95**, 4948–4951.
13. Also see Sevov, S C. and Corbett, J D , *Science*, 1993, **262**, 880–883 This is the only example of stuffed fullerene structure that we have come across. In these carbon-free fullerenes the bonding is not predominantly covalent
14 Jemmis, E D and Pavan Kumar, P. N. V., *Proc Indian Acad Sci (Chem Sci)*, 1984, **93**, 479–489.
15 Fajan, P. J , Calabrese, J. C. and Malone, B., *Acc. Chem. Res.*, 1992, **25**, 134–139
16 Wunderlich, J A and Lipscomb, W. N , *J Am Chem Soc* , 1960, **82**, 4427–4428
17 Hughes, R E , Kennard, C. H L , Sullenger, D. H , Weakliem, H. A , Sands, D. E. and Hoard, J L., *J Am Chem Soc* , 1963, **85**, 361–362.
18 Bakowies, D and Thiel, W., *J Am Chem Soc* , 1991, **113**, 3704–3714 The distance between the centroid of the C_{60} to the centre of one of the five-membered rings is calculated from the data in the above reference to be 3 33 Å The corresponding distance in Si_{60} is 5 15 Å[24]
19 Similarly centroid to the boron distance in $B_{12}H_{12}^{-2}$ is calculated to be 1 68 Å from ref. 16.
20 B–B distance in planar B_2H_4 (D_{2h}) calculated at the 6-31G* level is 1 76 Å.
21. Mass spectrometrically Si_{60}^+ was characterized to have a layered structure, see Zybill, C., *Angew Chem. Int. Ed Engl.*, 1992, **31**, 173–174 Even though fullerene-like Si_{60} has not been realized experimentally, theoretical predictions gave an impetus to take advantage of its size for stuffing, see ref 24
22 B–Si distance in planar BH_2SiH_3 is estimated as 2 22 Å see Mains, G. J , Bock, C. W. and Trachtman, M , *J Phys Chem* , 1989, **93**, 1745–1748
23 MNDO calculations on $B_2Si_4H_6$ gives the distance as 1 50 Å Dewar, M J S and Thiel, W , *J Am Chem Soc* , 1977, **99**, 4899–4906
24 Picqueras, M. C , Crespo, R., Orti, E and Tomias, F., *Chem Phys. Lett* , 1993, **213**, 509–513.

ACKNOWLEDGEMENT. B K. thanks CSIR, New Delhi for a research fellowship

Received 2 December 1993, revised accepted 5 March 1994.

Direct numerical simulation of a complex turbulent flow

M. D. Deshpande and P. N. Shankar

Computational & Theoretical Fluid Dynamics Division, National Aerospace Laboratories, Bangalore 560 017, India

Direct numerical simulations (DNS) have been carried out of the viscous, unsteady flow in a three-dimensional cavity generated by the motion of one of its walls. These flows are known to be complex and difficult to compute even when the Reynolds numbers are low enough to permit steady, laminar flow in the cavity. We have now been successful in computing unsteady, transitional and turbulent flows in this geometry. At Reynolds numbers of 3200 and 10,000 our computations show excellent agreement with the experimental data of Prasad and Koseff[1].

ALTHOUGH the equations governing the motion of a viscous, incompressible fluid, the Navier-Stokes equations, have been known for almost two centuries, very few complete solutions of these exist for realistic geometries. The difficulties stem from the essential nonlinearity of the equations and the wealth of possible phenomena, including turbulence, that can take place as a parameter Re, the Reynolds number, varies from zero to infinity. Till recently one could only resort, apart from experiments, to approximate methods, perturbation techniques and empirical and semi-empirical analysis. The availability of fast computers has, however, changed the scenario and it is now possible to accurately compute some complex, realistic flows for modest Reynolds numbers. This communication is to report such a computation which is somewhat special as detailed experimental results exist for this case with which the computational results can be compared.

We consider a viscous liquid completely filling a cubical cavity of side l_0; the fluid is set in motion by the uniform motion, at speed v_0, of the top wall along the direction of one of the generators of that wall, the y-direction. Let x be the depthwise coordinate and z the lateral or spanwise coordinate. Then the motion of the initially quiescent fluid is governed by the continuity equation and the N-S equations[2] in dimensionless form

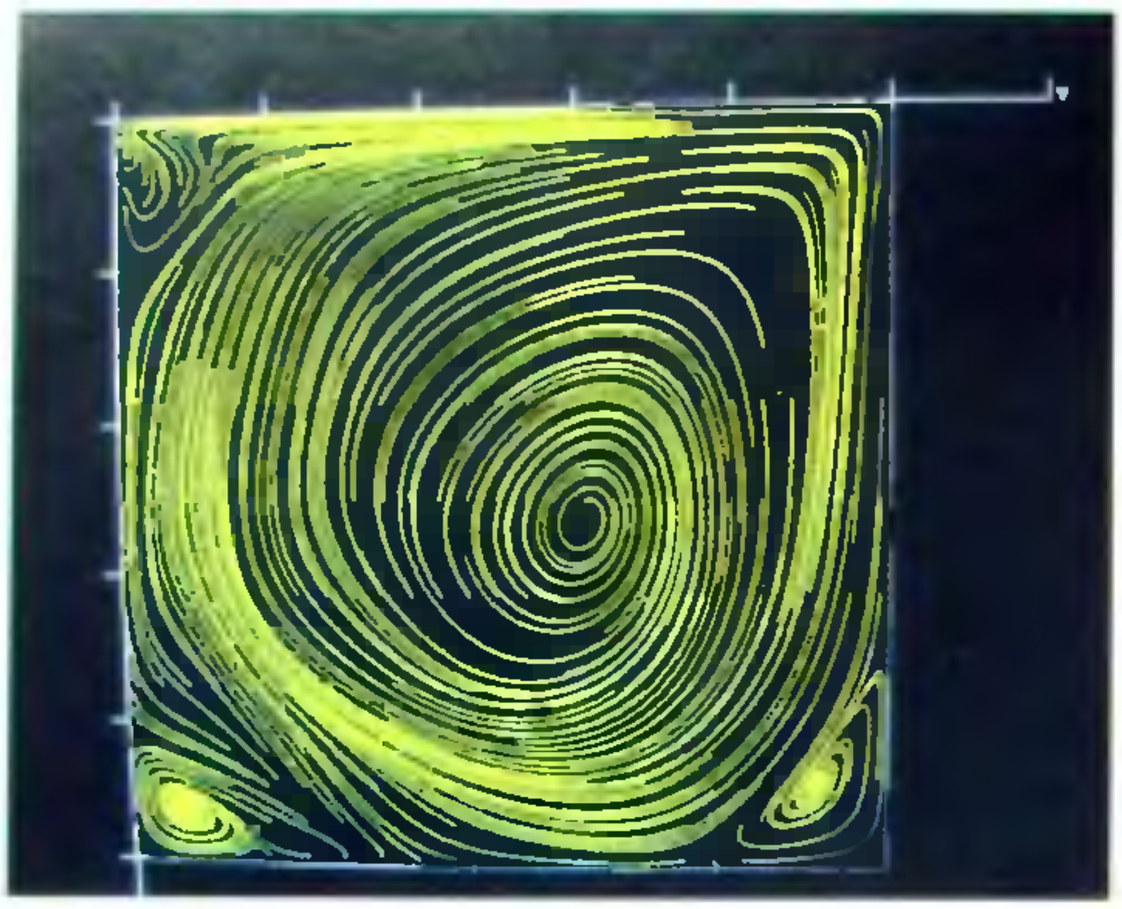

Figure 1. Instantaneous streamline pattern in the plane of symmetry, $Z = 0.5$. The top plate moves from left to right. Re = 3200

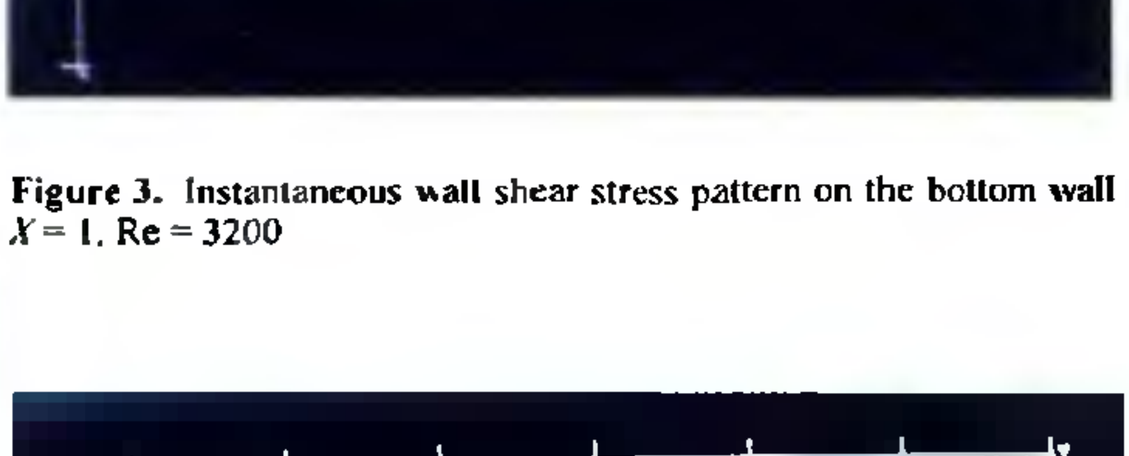

Figure 3. Instantaneous wall shear stress pattern on the bottom wall $Y = 1$. Re = 3200

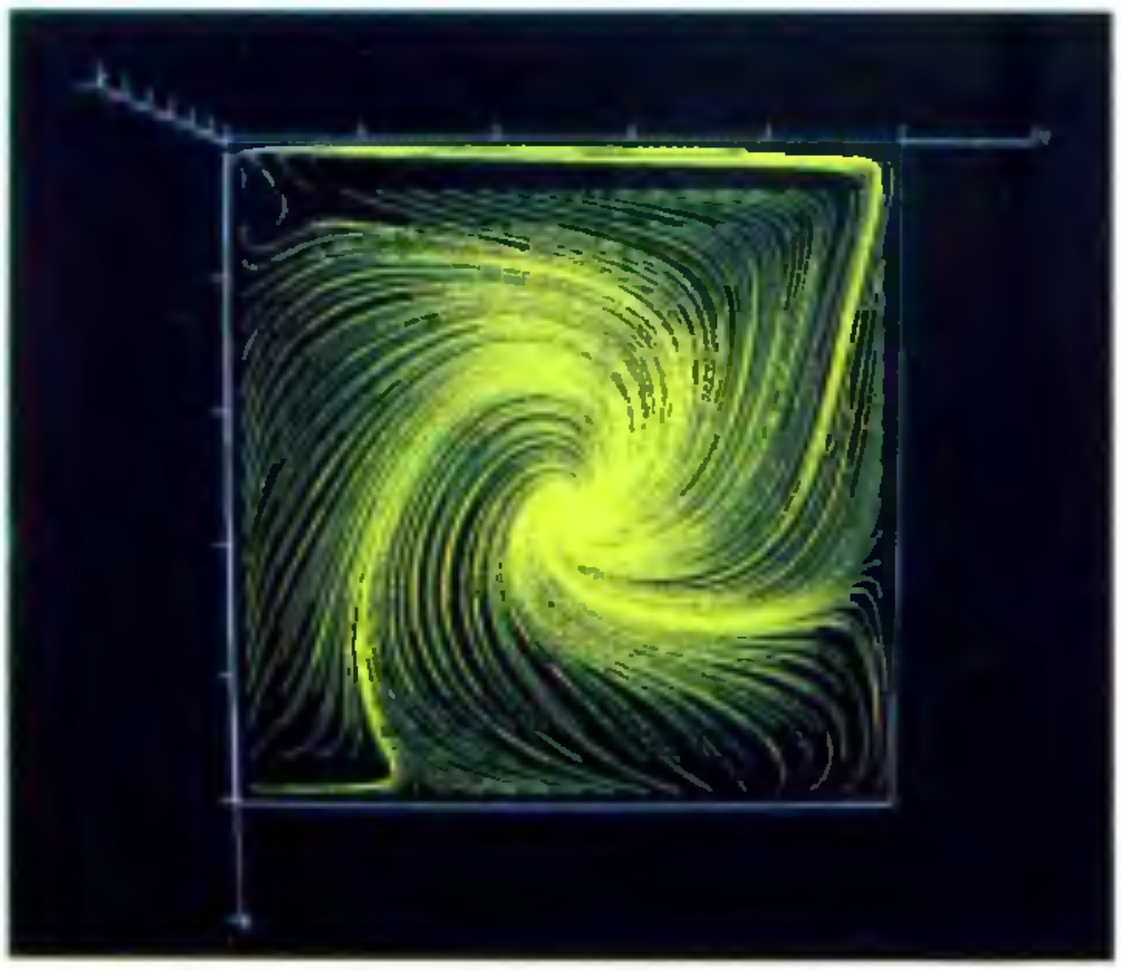

Figure 2. Instantaneous wall shear stress pattern on the endwall $Z = 0$. Re = 3200

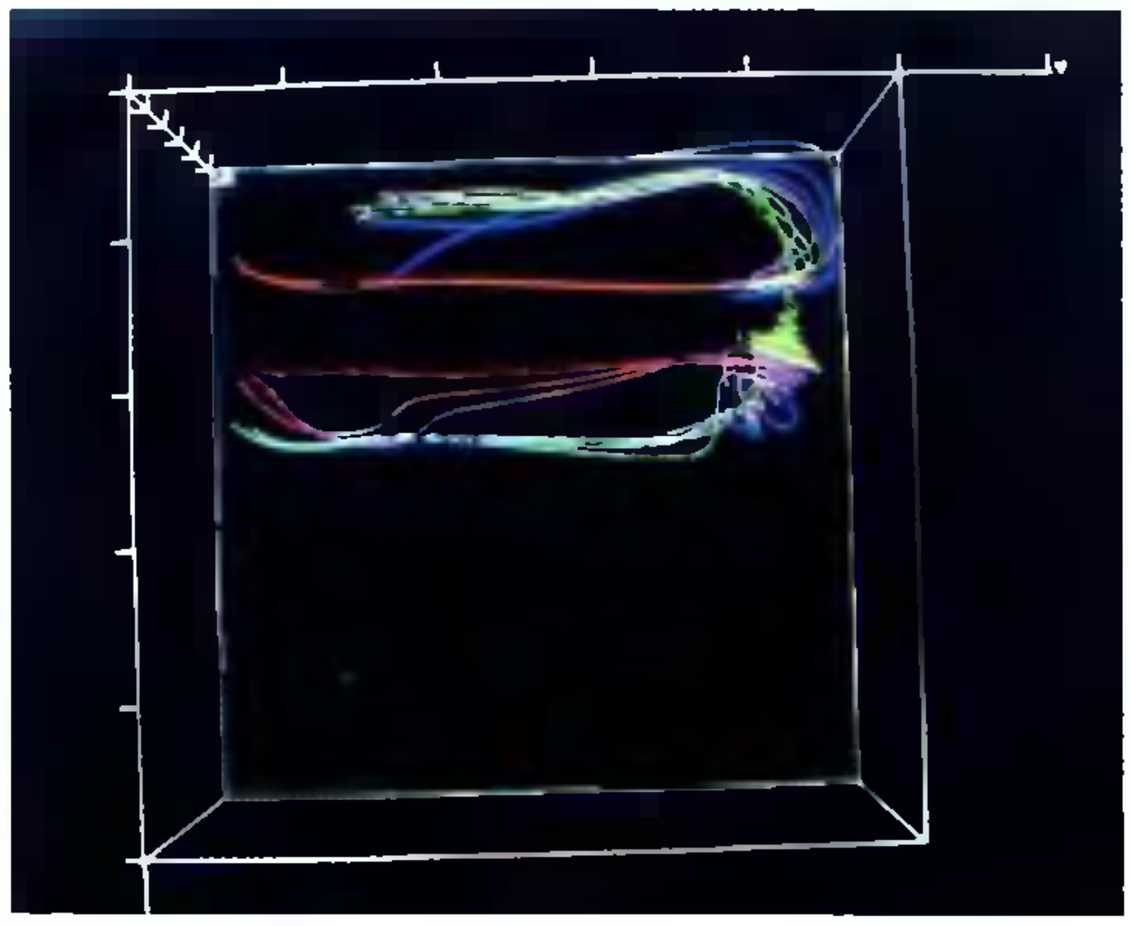

Figure 4. Plan view of the trajectories of tracer particles showing the complex particle paths followed. Re = 3200.

$$\nabla \cdot \vec{V} = 0,$$

$$\frac{\partial \vec{V}}{\partial \tau} + (\vec{V} \cdot \nabla)\vec{V} = -\nabla P + \mathrm{Re}^{-1} \nabla^2 \vec{V},$$

where $\vec{V}$ and P are the dimensionless fluid velocity and pressure respectively and $\mathrm{Re} = v_0 l_0 / \nu$ is the Reynolds number. The boundary conditions are that $\vec{V}$ has to vanish on the stationary walls and equal (0, 1, 0) on the moving upper wall. We have solved this system of equations by a finite difference method employing a third order upwind scheme[3]. The grid used was $84 \times 84 \times 84$, i.e. the field included more than a half a million grid points.

It is well known[3–5] that even at lower Reynolds numbers the flow in the cavity is complex. For $\mathrm{Re} \leq 1000$ the flow field is steady but highly three-dimensional with downstream and upstream eddies at

the bottom wall and corner eddies near the end walls in addition to the main primary eddy. At slightly higher Reynolds numbers longitudinal vortices, called Taylor–Goertler-like by Koseff and Street[4], make their appearance and the flow becomes unsteady. Although we have successfully simulated all these phenomena we restrict ourselves here to our computations of transitional and turbulent flows. This is because these are the flows of greatest theoretical interest and the most difficult to compute. At Re = 3200 the flow field is unsteady and the velocity traces at some locations in the field look qualitatively like those found in turbulent flows. We might classify this flow as a transitional flow. Figures 1–4 show various features of this interesting unsteady, three-dimensional flow field at this Reynolds number. Figure 1 shows the instantaneous streamline pattern at some instant in the symmetry plane ($Z = 0.5$) of the cavity. Apart from the main eddy, the upstream and downstream eddies at the bottom and an upper upstream eddy are clearly visible. Figures 2 and 3 show the instantaneous wall shear stress patterns on the endwall $Z = 0$ and the bottom wall $X = 1$. The spiral pattern in Figure 2 clearly shows that cross flows from the end walls feed the core of the main eddy. Figure 3 shows what might be seen if one looked down on the bottom wall and if the adjacent fluid had tracers in it. The downstream separation can be clearly seen on the right while the upstream eddy on the left is more convoluted. The most striking features though are the longitudinal patterns made by the TG vortices. Those familiar with critical point analysis[6] will recognize in Figures 2 and 3 nice examples of features such as foci and nodes. Figure 4 shows, again in plan, the motion of a number of tracer particles released close to an endwall and near the plane of symmetry respectively. Note the complicated spiralling motion near the downstream eddy.

Although the above qualitative results are of great interest our real success has been in the quantitative results of the computations. One of the reasons for this choice of geometry on our part had been the availability of very careful measurements by Prasad and Koseff[1]. We have compared our results at Re = 3200 and Re = 10,000 with all their data at these Reynolds numbers and find very good overall agreement. Figure 5 shows such a comparison for U_{rms} on the horizontal line of symmetry in the symmetry plane ($Z = 0.5$) for Re = 3200. Figure 6 shows a comparison for turbulent flow, at Re = 10,000, for $\overline{V}$ along the vertical line of symmetry in the same plane. It can be seen that the comparisons are very satisfactory. We have also compared our results for the Reynolds stresses and other mean and rms quantities and these compare very favourably. These detailed comparisons will be reported in a paper[7] to a specialist journal that is being submitted shortly. We must emphasize that our computations are a DNS, i.e. we use no adjustable parameters or fudge factors. To the best of our knowledge the present computations represent one of the most direct and stiff tests of a DNS and the results have been most gratifying.

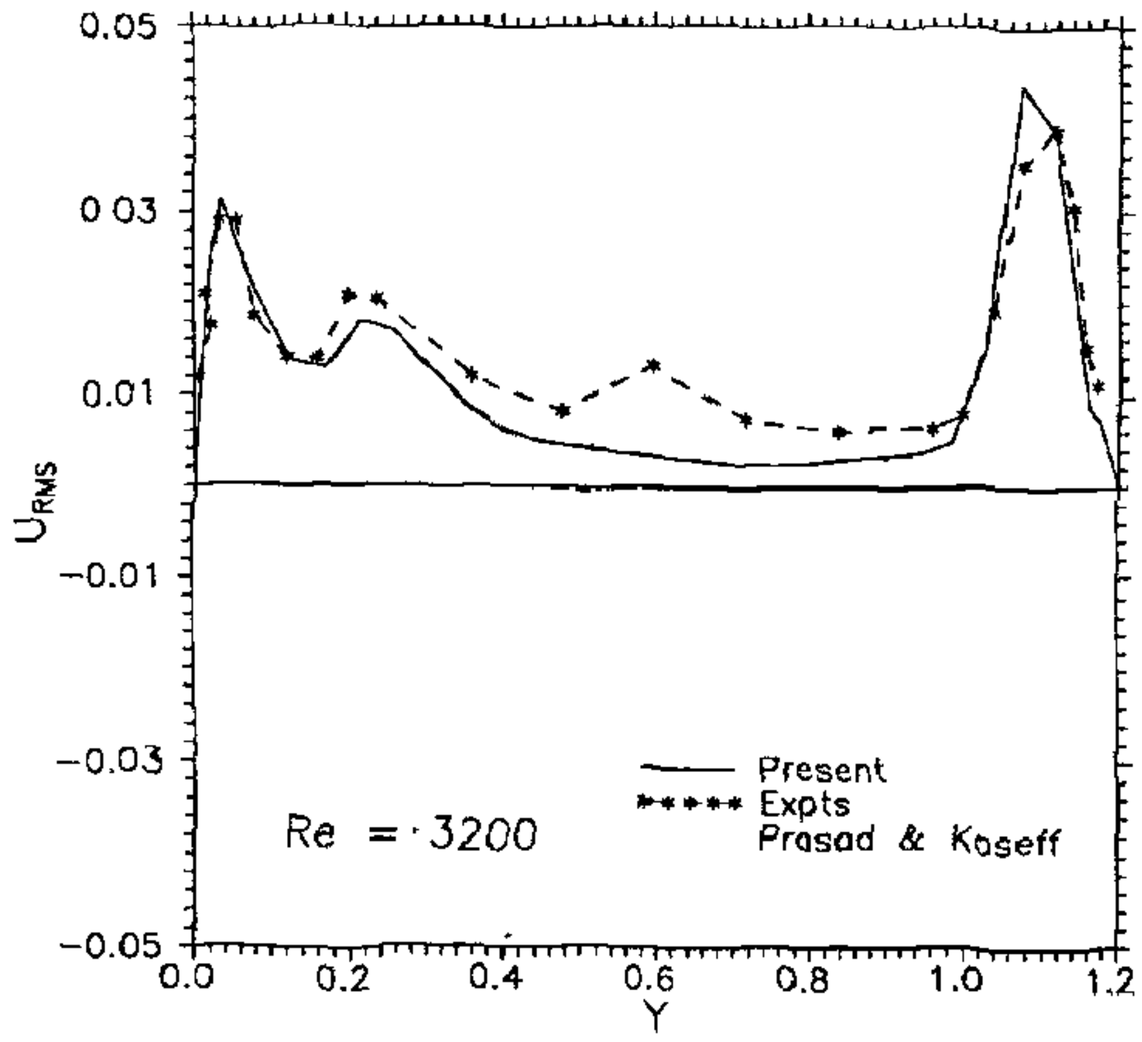

Figure 5. Comparison of the results of the computations with experimental results at Re = 3200. U_{rms} is plotted as a function of Y at $X = 0.5$ in the symmetry plane.

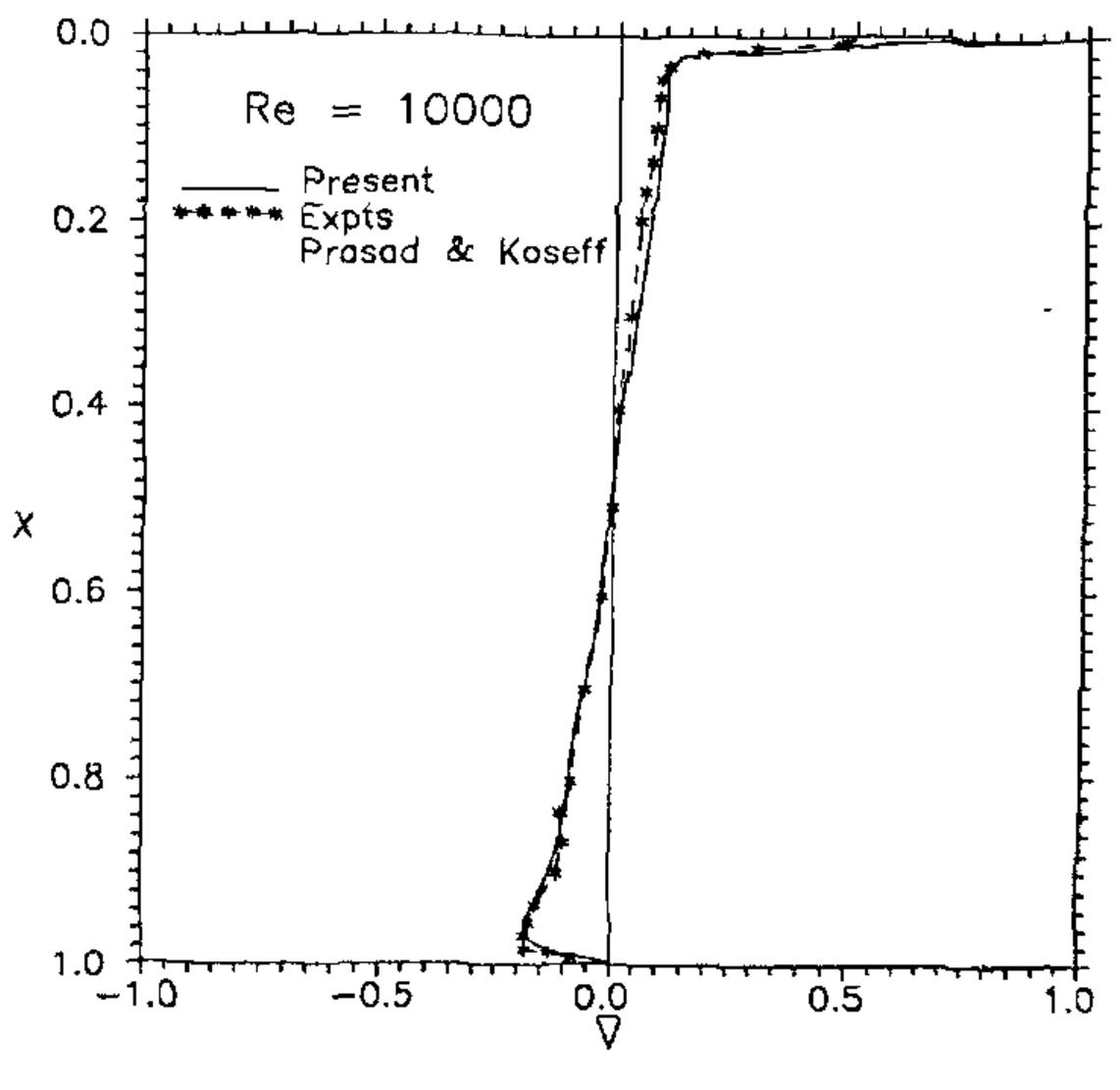

Figure 6. Comparison with experiments at Re = 10,000. $\overline{V}$ is plotted against X at $Y = 0.5$ in the symmetry plane.

1 Prasad, A. K. and Koseff, J. R., *Phys. Fluids*, 1989, **A1**, 208
2 Batchelor, G. K., *An Introduction to Fluid Dynamics*, Cambridge University Press, 1967

3 Deshpande, M D , NAL Project Document, 1993, PD CF 9305.
4 Koseff, J R and Street, R L , *J Fluids Eng* , 1984, **106**, 390.
5 Ishii, K and Iwatsu, R , Proc IUTAM Symp. Cambridge, 1990.
6 Perry, A E and Chong, M S , *Annu. Rev Fluid Mech* , 1987, **19**, 125
7 Deshpande, M D and Shankar, P N , to be submitted to *J. Fluid Mech* , 1994

ACKNOWLEDGEMENTS We thank Dr S George Milton and Mr S Balaji for the considerable assistance they provided in computing, data reduction and computer graphics We also gratefully acknowledge financial support from AR&DB under grant No 685

Received 11 February 1994, accepted 21 February 1994

Luminescence chronology of a fossil dune at Budha Pushkar, Thar Desert: Palaeoenvironmental and archaeological implications

A. K. Singhvi*, D. Banerjee*, S. N. Rajaguru and V. S. Kishan Kumar*†**

*Physical Research Laboratory, Ahmedabad 380 009, India
** Deccan College, Pune 411 006, India
† Arid Forest Research Institute, Jodhpur 342 008, India

Chronological studies on a fossil dune at Budha Pushkar in Thar desert suggest that the existing hypothesis of a *wetter* Middle Palaeolithic period in the region is not tenable. The present study suggests a revision of the stratigraphic framework of this regionally correlatable sequence in the Thar desert and questions the earlier archaeological inferences.

IT is now well established that several dune-sections in the marginal areas of Thar Desert have preserved a long record of Early Man and Environmental Change[1–3]. The intermontane dune sequence at the fringe of the freshwater lake Budha Pushkar (74°36'E, 26°30'N.) is an important geoarchaeological site that has been extensively studied and eloquently debated. The debate ranges from basic differences on the stratigraphic locations of various sub-horizons to the association and typologic classification of lithic artefacts within various aeolian/palaeosoil sub-units. Even more contentious has been the controversy on the presence of a 'Rotlehm'-type red-brown soil and its interpretation on the amplitude of environmental change. This controversy still persists due to lack of a chronological framework which so far has been limited to a few radiocarbon dates on pedogenic calcrete nodules of somewhat dubious validity[4]. We describe here the results of a detailed luminescence dating programme and discuss its bearing on the previously suggested timing and amplitude of palaeoenvironmental changes in the Thar during the late Quaternary.

Pioneering studies by Allchin *et al.*[1, 2] led to the discovery of several Stone Age sites, particularly in the context of aeolian stratigraphy of the Thar desert. At Budha Pushkar, the authors reported the presence of Lower-, Middle-, Upper-Palaeolithic artefacts and Mesolithic tools and used these to ascribe chronology to their deductions on the environmental change. Based on the presence of a dark-brown 'Rotlehm' type soil along with a proliferation of Middle Palaeolithic artefacts, the authors suggested that during the Middle Palaeolithic period, the Thar witnessed a major wet-phase, especially since this red-brown soil was traceable to sites in the South (Pawagarh) as well. Agrawal *et al.*[4] and Wasson *et al.*[5] however, indicated that the ages based on Middle Palaeolithic artefacts could not be used since they occurred only on the surface of reddish brown dune and not in the dune matrix. They also doubted the cultural assignment of these artefacts since invariably the larger artefacts were found in association with the microliths. Chemical studies by Agrawal *et al.*[4] further indicated that the horizon designated as 'Rotlehm' soil was alkaline and did not show any convincing evidence of strong leaching and that the pedogenesis merely consisted of a marginal organic accumulation (< 1%), iron oxidation and a rather weak carbonate leaching. Based on these facts, the very designation of the horizon as Rotlehm soil was questioned with an implicit bearing on the deductions on climatic change. More recent micromorphological studies on the red-soil horizon by Achyuthan and Rajaguru[6] have indicated the presence of easily weathered minerals such as hornblende and plagioclase, which also suggest absence of any intense weathering. The authors argue that the soil only represents a weak weathering that suggests a semi-arid climatic regime. Figure 1 provides the general stratigraphy as suggested by Allchin *et al.*[1, 2] and as deduced by one of the present authors (S. N. Rajaguru).

The dune-sands were dated using the luminescence dating method[7, 8]. The experimental procedure was identical to that described by Chawla *et al.*[9] with the following variations:

(i) The purity of 106–150 μm quartz grains was checked using an 880 nm infra-red stimulated luminescence system (IRSL) and only the samples that did not exhibit an IRSL were chosen. Samples exhibiting IRSL were retreated with 40% HF for 10 min.
(ii) TL analysis was made using a Schott UG-11 filter that enabled an isolation of optically easy-to-bleach 325°C glow-peak of quartz[10].
(iii) The equivalent doses were estimated using the total bleach method[7], the total bleach-regeneration method[11, 12] and the partial bleach method[13]. In the total bleach method, two bleaching times of 30 min and 13 h